

# Implementation of the Incremental Conductance MPPT Algorithm for Photovoltaic Systems

Srdjan Srdic, Zoran Radakovic  
 School of Electrical Engineering  
 University of Belgrade  
 Belgrade, Serbia  
 srdic@etf.rs, radakovic@etf.rs

Vladimir Vojinovic  
 Al Pack d.o.o.  
 Subotica, Serbia  
 vlakietf@gmail.com

**Abstract**—An implementation of the Incremental Conductance (INC) Maximum Power Point Tracking (MPPT) algorithm for photovoltaic systems is presented in this paper. The MPPT algorithm was implemented on a boost converter, which was meant to operate as an input stage of a single-phase transformerless grid connected photovoltaic (PV) converter. The implementation of the algorithm has been divided into two steps. The first step was to simulate the tracker's operation under fast changing solar irradiance conditions, by using the appropriate simplified models of the dc/dc converter and the PV string. The second step was to implement the obtained optimized control parameters on a hardware setup consisting of a 1 kW boost converter prototype and a fast prototyping DSP platform board. During the testing phase, several problems were encountered and successfully solved. The performance of the algorithm was evaluated by simulations, and the simulation results were successfully verified on the hardware prototype.

**Keywords:** incremental conductance, maximum power point tracking, photovoltaic systems, power generation control

## I. INTRODUCTION

The generation of the electric energy from sunlight by PV panels is a very attractive way of producing energy from a practically unlimited energy source. Apart from the fact that the fuel is free and available everywhere in the world, the generation of the electricity by PV panels has some additional merits: it is nonpolluting, noiseless and requires very little maintenance. However, despite the aforementioned advantages, the efficiency of solar power systems is low (the efficiency of PV panels is up to 20% [1]) and depends on many factors such as temperature, solar irradiance, dirt, shadows, and so on [2]. The current-voltage characteristic of a solar panel is nonlinear, and the generated power has its maximum at a certain operating point, called the Maximum Power Point (MPP), as shown in Fig. 1. In Fig. 1,  $I_{SC}$  is the panel short-circuit current, and the  $U_{OC}$  is the panel open-circuit voltage.

Therefore, in order to generate as much energy as possible at given operating conditions, the PV panel should operate at its MPP, i.e. the energy should be generated with the highest power available. Since the MPP changes with the solar irradiation and the ambient temperature, an algorithm which performs a Maximum Power Point Tracking is necessary.

Ideally, by employing a MPPT algorithm, the PV panel output power is maximized regardless of the solar irradiance, the ambient temperature, and varying atmospheric conditions. As a consequence, the efficiency of the power generation is increased, as well as the amount of the generated energy.

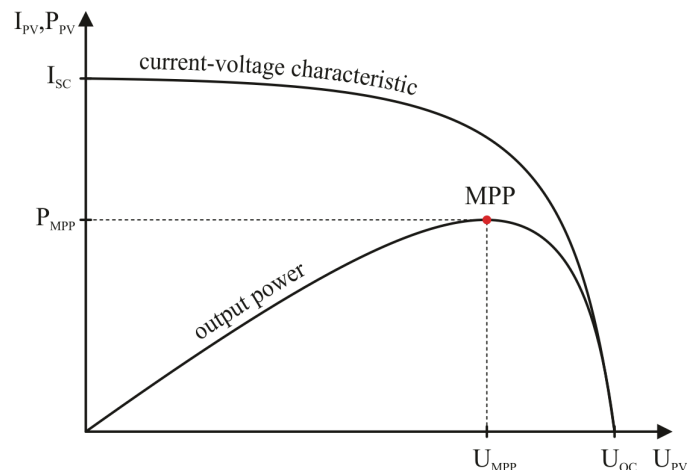


Figure 1. A current-voltage characteristic of a PV panel, an output power characteristic and the maximum power point.

There are more than fifteen methods for tracking the maximum power point [3], but the following three are most widely used [4]:

- Constant Voltage (CV)
- Perturb and Observe (P&O)
- Incremental Conductance (INC)

The CV method relies simply on the fact that the ratio  $U_{MPP}/U_{OC}$  is nearly constant, i.e.  $U_{MPP}/U_{OC} \approx k$  [5]. Although the CV algorithm is very simple, it is difficult to choose the optimal value for the constant  $k$ . According to [5] optimal value of  $k$  is in the range from 73% to 80%. Another problem with this method is that  $k$  actually depends on temperature and irradiance, and can vary by as much as 8% over the entire range of operating conditions.

The P&O method is widely used MPPT method due to its simplicity. In the P&O algorithm, the PV panel voltage is

periodically perturbed (increased or decreased), and the panel output power is being monitored after each perturbation. If the output power increases after a perturbation, the next perturbation should be made in the same direction as the previous one. If the power decreases, the perturbation should be made in the opposite direction. The algorithm will continue to perturb the PV panel voltage even after the MPP has been reached. Thus, after the MPP has been reached, the PV panel voltage will oscillate around the maximum power point. These oscillations will result in an unwanted loss of PV power, and reduced system efficiency. The oscillations could be minimized by reducing the perturbation step size. However, reduction of the step size would slow down the MPPT. Another limitation of the P&O algorithm appears during low insolation levels, when panel power curve tends to flatten out. This makes it difficult for the algorithm to discern the location of the MPP, since the changes of the output power are small with respect to the voltage change. Also, in the case of rapidly changing atmospheric conditions (e.g. fast moving clouds), the P&O algorithm will deviate from the MPP until the changes slow down. This is because the P&O algorithm assumes that the PV power changes are a result of the panel voltage perturbations only [2]-[5]. This behavior is illustrated in Fig. 2.

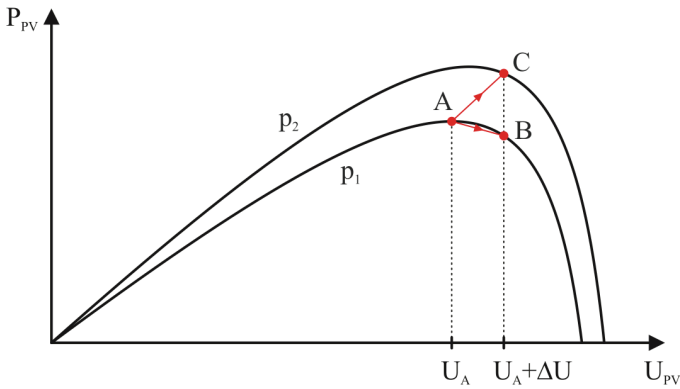


Figure 2. The divergence of the operating point from the MPP, for the P&O algorithm under rapidly changing atmospheric conditions.

As shown in Fig. 2, for a positive perturbation of the panel voltage (from  $U_A$  to  $U_A + \Delta U$ ), the operating point will move from A to B on the curve  $p_1$  if the atmospheric conditions stay approximately constant during one sampling period. As a result, the panel output power will decrease. Therefore, the next perturbation will be made in the opposite direction, and the operating point will be moved towards the MPP. However, if the irradiance increases during one sampling period (i.e. the power curve shifts from  $p_1$  to  $p_2$ ), the operating point will move from A to C, for the same perturbation of the panel voltage from  $U_A$  to  $U_A + \Delta U$ . As a result of this perturbation, the output power will increase. Now, since the output power has increased, the next perturbation will be made in the same direction (the panel voltage will be increased again), and the operating point will move further away from the MPP. The operating point will continue to diverge from the MPP if the irradiance continues to increase. In order to prevent panel voltage oscillations due to the rapid irradiance changes, the three-point weight P&O algorithm was introduced in [6]. This algorithm performs the tracking based on the measurements in

the three operating points: the current point (e.g. point X), the point Y (which is point X plus one positive perturbation), and the point Z (which is point Y plus two negative perturbations). This algorithm essentially prevents PV panel voltage changes in the case when solar irradiance changes rapidly, thus preventing the unwanted panel voltage oscillations.

In order to overcome the drawbacks of the classical P&O MPPT algorithm, the Incremental Conductance algorithm is introduced. Unlike the P&O algorithm, the INC algorithm always compares the PV panel voltage with the MPP voltage and it does not oscillate around the MPP. Therefore, it is more efficient than the classical P&O algorithm [5], [7].

## II. DESCRIPTION OF THE IMPLEMENTED ALGORITHM

The incremental conductance method is based on a fact that the slope of the output power curve of the solar panel is equal to zero at the point of the maximal power, as shown in Fig. 1 [7]. The slope is positive to the left of the MPP, and negative to the right of the MPP. Thus, the following equations are valid:

$$\begin{aligned} \frac{dP_{PV}}{dU_{PV}} &= 0 \quad , \quad \text{at the MPP} \\ \frac{dP_{PV}}{dU_{PV}} &> 0 \quad , \quad \text{to the left of the MPP} \\ \frac{dP_{PV}}{dU_{PV}} &< 0 \quad , \quad \text{to the right of the MPP} \end{aligned} \quad (1)$$

Since the panel output power is a product of the PV output voltage,  $U_{PV}$ , and the PV output current,  $I_{PV}$ , the following holds:

$$\frac{dP_{PV}}{dU_{PV}} = \frac{d(U_{PV} I_{PV})}{dU_{PV}} = I_{PV} + U_{PV} \frac{dI_{PV}}{dU_{PV}} \cong I_{PV} + U_{PV} \frac{\Delta I_{PV}}{\Delta U_{PV}} \quad (2)$$

The equations (1) now become

$$\begin{aligned} \frac{\Delta I_{PV}}{\Delta U_{PV}} &= -\frac{I_{PV}}{U_{PV}} \quad , \quad \text{at the MPP} \\ \frac{\Delta I_{PV}}{\Delta U_{PV}} &> -\frac{I_{PV}}{U_{PV}} \quad , \quad \text{to the left of the MPP} \\ \frac{\Delta I_{PV}}{\Delta U_{PV}} &< -\frac{I_{PV}}{U_{PV}} \quad , \quad \text{to the right of the MPP} \end{aligned} \quad (3)$$

As stated in [8] (where the INC method is introduced for the first time), at the MPP, the slope of the tangent to the current-voltage curve is equal to that of the line passing through the points  $(U_{OC}, 0)$  and  $(0, I_{SC})$  (shown in Fig. 1). Since the first equation in (3) is independent of the shape of the current-voltage curve, it holds valid irrespective to the current-voltage curve changes. As in the case of P&O algorithm, the basic INC algorithm also requires measurements of PV voltage and current in order to perform the MPP tracking.

The basic fixed step INC MPPT algorithm is based on equations (3), and the flowchart for the algorithm was shown in Fig. 3. In Fig. 3,  $U_k$  and  $I_k$  are k-th sample of the panel voltage,  $U_{PV}$ , and the panel current,  $I_{PV}$ , respectively.  $U_r$  is a PV setpoint

voltage, and  $\Delta U_r$  is a setpoint step change (which is fixed). The setpoint step change determines the speed of the algorithm, i.e. how fast the algorithm would track the MPP. By choosing the larger voltage setpoint step change, the algorithm would track the MPP faster, but at the same time the unwanted oscillations around the MPP can occur [3].

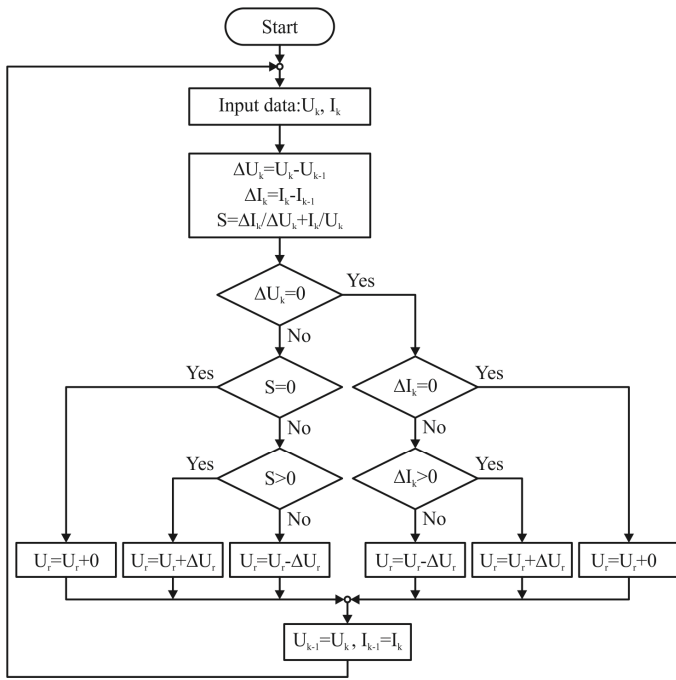


Figure 3. The flowchart for the basic INC MPPT algorithm.

The algorithm starts by sampling the panel voltage and the current. It then calculates the incremental changes of the panel voltage and the current by subtracting the values sampled at the previous MPPT cycle from the new ones. At the same time, the algorithm calculates the sum of the incremental conductance,  $\Delta I_k / \Delta U_k$ , and the instantaneous conductance,  $I_k / U_k$ . The sign of the calculated sum  $S$  is then checked, and a new setpoint is determined in order to move the panel voltage towards the MPP. At the MPP, the sum  $S$  is equal to zero, and no further action is needed. If the MPP was reached in the previous cycle, the algorithm checks the sign of the panel current change in order to determine further actions. If the panel current has changed due to a change in the atmospheric conditions, the algorithm will adjust the setpoint so that the panel voltage will be moved towards the MPP.

In the described algorithm, the voltage and the current changes, as well as the sum  $S$ , are compared to zero. In practical application, those conditions will hardly be fulfilled due to made approximation  $dX \approx \Delta X$  and due to measurement and quantization errors during the sampling process. In order to take this into account, the basic algorithm needs to be changed to allow some marginal error. The value of the allowed error depends on the required sensitivity of the algorithm [7].

The flowchart for the enhanced algorithm was shown in Fig. 4. The introduced error margins  $\epsilon_U$ ,  $\epsilon_I$ , and  $\epsilon_{INC}$ , shown in Fig. 4, were set to the following values:  $\epsilon_U=0.3$ ,  $\epsilon_I=0.01$ , and  $\epsilon_{INC}=0.001$ . Also, the voltage setpoint step change was set to

$\Delta U_r=5V$ . All these values were determined during the testing of the algorithm.

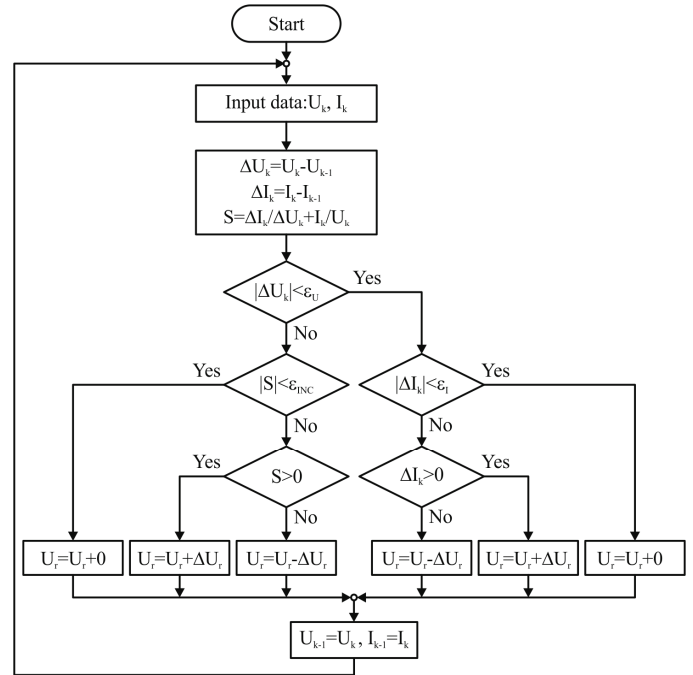


Figure 4. The flowchart for the enhanced INC MPPT algorithm.

Based on the enhanced INC algorithm, the appropriate Simulink model of the algorithm was created and the algorithm was later implemented on the hardware prototype.

### III. DESCRIPTION OF THE LABORATORY SETUP

The laboratory setup on which the tracker operation is evaluated consists of a simplified model of the PV string and a 1 kW boost converter prototype, as shown in Fig. 5.

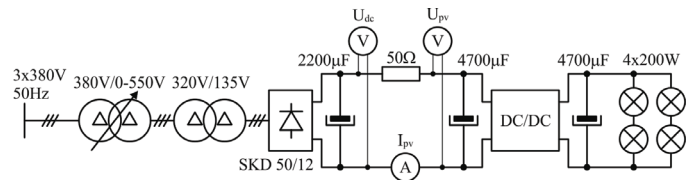


Figure 5. The schematic of the laboratory setup.

The boost converter is meant to be a part of a grid-connected photovoltaic system, in which its input is connected to a PV string, and its output is connected to a single-phase inverter through a dc-link capacitor circuit. The boost converter is meant to operate with the input voltage in the range from 150 V to 350 V, and the constant output voltage of 400 V. The converter output voltage is maintained constant by the inverter. However, during the testing of the MPP tracker, a simple resistive load (light bulbs) was connected to the boost converter output, instead of an inverter (the inverter prototype has not yet been developed at the time of the MPPT testing). As shown in Fig. 5, the four 200 W light bulbs are used as a load. An additional electrolytic capacitor is connected parallel to the bulbs, acting as the dc-link capacitor and preventing fast

oscillations of the output voltage, which could negatively influence the tracker performance.

In order to test the implemented MPPT algorithm under rapid solar irradiance change conditions, a simplified model of the PV string (consisting of the series connection of the variable dc voltage source ( $U_{dc}$ ) and the resistor of fixed resistance of  $50 \Omega$ ) was built, instead of using an actual PV string. The current-voltage characteristic of such a source is linear, and the power-voltage characteristic is parabola, with the maximum power occurring when  $U_{pv}$  voltage is half the  $U_{dc}$  voltage, as shown in Fig. 6. The  $U_{pv}$  and  $U_{dc}$  are measured at points shown in Fig. 5. Thus, the change in the irradiance is modeled by changing the  $U_{dc}$  voltage, as shown in Fig. 6, where a power curve  $p_1$  corresponds to a case of lower irradiance and a curve  $p_2$  to a case of higher irradiance. It can be noticed that the power curves shown in Fig. 6 are similar to the curves shown in Fig. 2.

According to the basic circuit theory, the maximum power at the terminals of a series connection of the voltage source and the resistor, will occur when the voltage at the terminals is half the voltage of the voltage source (i.e. half the open-circuit voltage of the series connection). Therefore, in order to evaluate the MPPT algorithm operation, the dc source voltage,  $U_{dc}$ , (see Fig. 5 and Fig. 6) will be changed, and the  $U_{pv}$  voltage will be monitored. If, after the  $U_{dc}$  change,  $U_{pv}$  voltage settles at  $U_{dc}/2$ , then the MPP tracker operates correctly, i.e. tracks the maximum power point, as shown in Fig. 6.

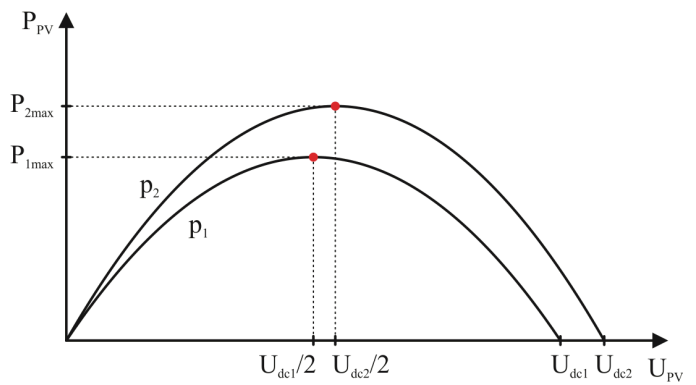


Figure 6. Output power vs. output voltage of a simplified model of the PV string.

#### IV. SIMULATION OF THE IMPLEMENTED ALGORITHM

In order to be able to experimentally verify the simulation results, the Simulink model of the power stage (made of blocks from MATLAB's "SimPowerSystems" library) corresponding to the laboratory setup was created.

The operation of the implemented algorithm is simulated and the simulation results were shown in Fig. 7. As can be seen in the Fig. 7, the implemented tracker tracks the MPP successfully. The tracker is set to operate (to change the setpoint voltage  $U_T$ ) with the period of 0.2048 s.

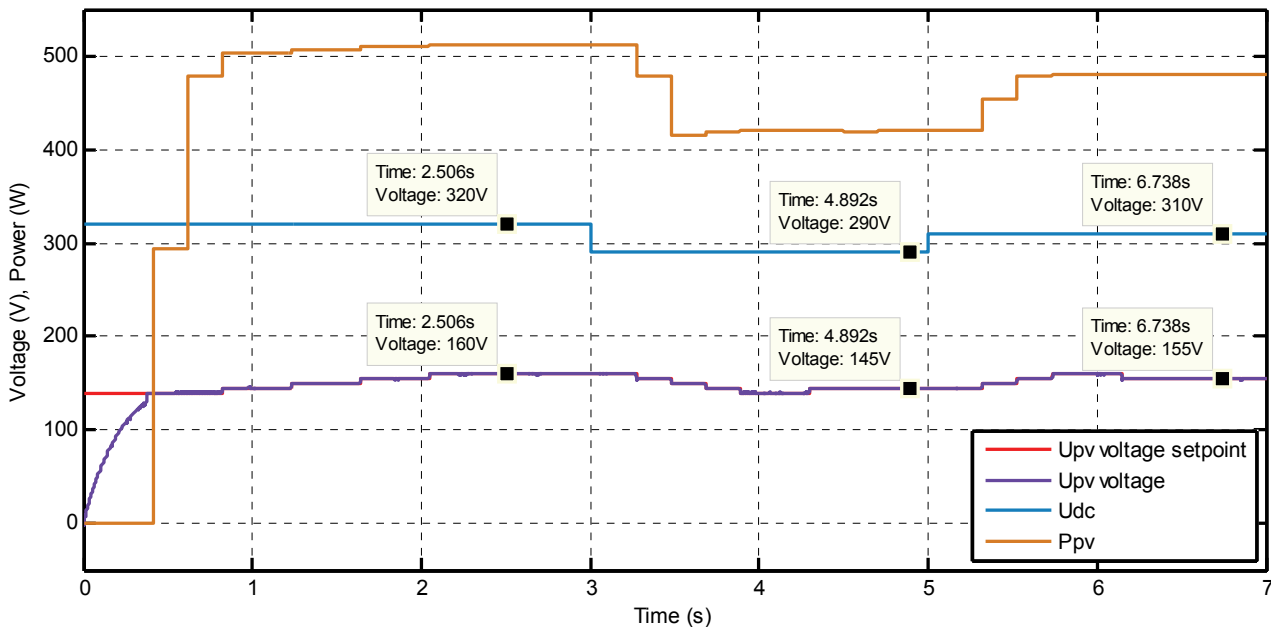


Figure 7. The implemented INC MPPT algorithm simulation results.

The PV string current and voltage were sampled every  $200 \mu s$ , and the average value of the 1024 samples is taken as the input to the tracker in every tracker cycle (values denoted as  $U_k$  and  $I_k$  in the flowcharts).

During the simulation process, the major problem was to properly tune the error margin coefficients  $\epsilon_U$ ,  $\epsilon_I$ , and  $\epsilon_{INC}$ .

These coefficients needed to be tuned in such a way that they enable proper operation of the tracker. In general, values for the  $\epsilon_U$  and  $\epsilon_I$  depend on the measurement noise and the adopted averaging interval (number of samples to be averaged). If these coefficients are too small, then, in the case of noisy current and voltage signals and/or short averaging intervals, the PV

voltage and/or current change can be falsely detected. That could lead to the erratic operation of the tracker. If the margins were set too large, then real changes of the string current and/or voltage would not be detected. The  $\epsilon_{INC}$  coefficient also needs to be properly tuned. If this coefficient is set too small, then, in low irradiance conditions, tracker may deviate from the MPP. Namely, in low irradiance conditions, in the range of voltages near  $U_{MPP}$ , the resulting change in power when the string voltage is changed is very small (because power characteristic is "flattened" in low irradiance conditions). Therefore, after a voltage change, the sum  $S$  can become lower than the  $\epsilon_{INC}$ , and the incremental conductance algorithm can get "stuck" at an operating voltage that is not quite the same as  $U_{MPP}$ . If, on the other hand, the  $\epsilon_{INC}$  is too large, the tracker will diverge from the MPP. After numerous simulations, the error margin coefficients values were determined and set to previously remarked values.

The determination of the voltage setpoint step change,  $\Delta U_r$ , was another important task during the simulation process. If a small step change was chosen, the response of the tracker would be slow. If the step change is large, the tracker would become inaccurate. The 5 V step was chosen as a result of a compromise between the speed and the accuracy of the tracker.

### V. EXPERIMENTAL EVALUATION OF THE IMPLEMENTED ALGORITHM

In order to implement the simulated algorithm on the hardware setup, the developed simulink model of the MPP algorithm had to be translated to the appropriate model by using blocks from the fixed-point library "C28x IQmath". The model was then converted to a Code Composer Studio project, from which the hex code was generated and ran on the TMS320F28027 development kit board.

One of the major problems during the experimental evaluation was the oscillating input current. The input current was oscillating at about 400 Hz due to the specific nature of the test setup (use of a three-phase rectifier as a source of the  $U_{dc}$  voltage). Since this current was used by the algorithm to compute the output power of a PV string, those unwanted oscillations needed to be mitigated. This was done by introducing a 4700 $\mu$ F capacitor in parallel to the input of the converter, as shown in Fig. 5. It should be noted that the conditions under which the controller was tested were less favorable than those in real-life application, because in real-life application the inverter (which is connected to the output of the boost converter) would keep the dc-link voltage at nearly a constant value of 400V. However, in the test setup, the boost converter output voltage was varying, and it was determined by the power balance between the input and the output of the converter. Also in real-life application the converter's input would be connected to the PV string, and the string current would not oscillate.

The operation of the implemented algorithm was experimentally verified by manually adjusting the dc source voltage,  $U_{dc}$ , and monitoring the changes of the  $U_{pv}$  voltage. The experimental results were shown in Fig. 8 and Fig. 9. In both figures, a cyan trace represents the dc source voltage,  $U_{dc}$ , while the orange trace represents the  $U_{pv}$  voltage.

In Fig. 8, the  $U_{dc}$  voltage was reduced from about 300 V to about 280 V. This voltage change corresponds to a rapid decrease of a solar irradiance. The tracker managed to track the MPP, and the  $U_{pv}$  voltage was changed from 150 V to 140 V, after a few cycles. In Fig. 9, the  $U_{dc}$  voltage was increased from about 285 V to about 310 V. This voltage change corresponds to a rapid increase of a solar irradiance. The tracker managed to track this change, and the  $U_{pv}$  voltage was changed from 140 V to 160 V, after a few cycles. However, in this case the tracker set the voltage setpoint 5 V above the theoretically correct MPP voltage value of 155 V. This error might be due to a relatively large setpoint step change and/or due to the averaging process of the noisy PV string current and voltage signals, and it is commonly observed in the fixed-step algorithms [9], [10]. The setpoint step change of 5 V, as well as the tracker cycle duration of 0.2048 s, are noticeable in both Figures.

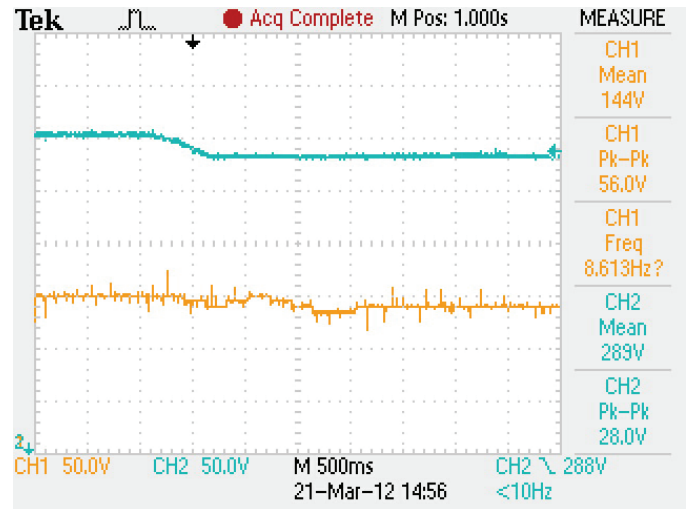


Figure 8. The MPP tracker operation after the reduction of the  $U_{dc}$  voltage from about 300 V to about 280 V.

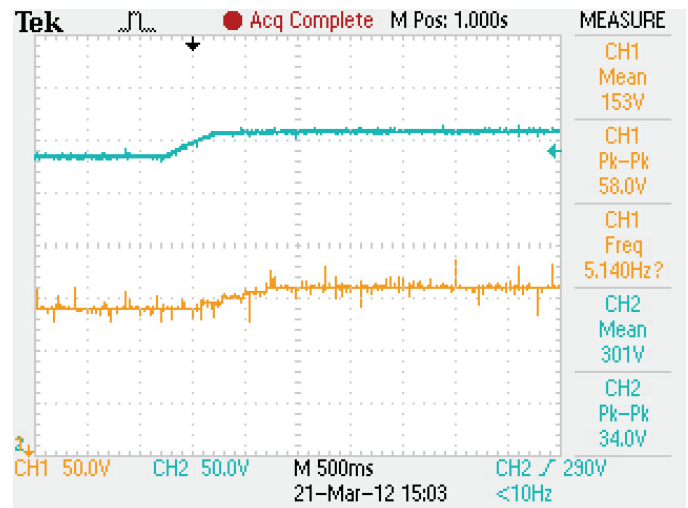


Figure 9. The MPP tracker operation after an increase of the  $U_{dc}$  voltage from about 285 V to about 310 V.

## VI. CONCLUSION

This paper presents the results of the implementation of the basic fixed step size Incremental Conductance MPPT algorithm on a 1 kW boost converter prototype. The tracker was tested under rapid solar irradiance change conditions by using a simplified model of the PV string (consisting of the series connection of the variable dc voltage source ( $U_{dc}$ ) and the resistor of fixed resistance of  $50 \Omega$ ) which enabled the emulation of the rapid changes of the solar irradiance. The error margin coefficients and the voltage setpoint step change in the algorithm were determined during the simulation process, and translated to the hardware prototype. Both the simulation and the experimental results showed a satisfactory tradeoff between the accuracy and the speed of the algorithm.

## REFERENCES

- [1] Sunpower corporation (2012, February 29). *SunPower E20/327 Residential Solar Panel*, Document #001-65484 Rev\*B / LTR\_EN [online]. Available: <http://us.sunpowercorp.com/homes/products-services/solar-panels/e20/>
- [2] A. Safari, S. Mekhilef, "Simulation and Hardware Implementation of Incremental Conductance MPPT With Direct Control Method Using Cuk Converter," *IEEE Transactions on Industrial Electronics*, vol.58, no.4, pp.1154–1161, April 2011.
- [3] T. Eram, P. L. Chapman, "Comparison of Photovoltaic Array Maximum Power Point Tracking Techniques," *IEEE Transactions on Energy Conversion*, vol.22, no.2, pp.439–449, June 2007.
- [4] D. Sera, T. Kerekes, R. Teodorescu, F. Blaabjerg, "Improved MPPT Algorithms for Rapidly Changing Environmental Conditions," *12th International Power Electronics and Motion Control Conference EPE-PEMC 2006*, pp.1614–1619, 30 Aug. – 1. Sept. 2006.
- [5] D. P. Hohm and M. E. Ropp, "Comparative Study of Maximum Power Point Tracking Algorithms," *Progress in Photovoltaics: Research and Applications*, vol. 11, issue 1, pp.47–62, Jan. 2003.
- [6] Ying-Tung Hsiao, China-Hong Chen, "Maximum power tracking for photovoltaic power system," *Conference Record of the Industry Applications Conference, 2002. 37th IAS Annual Meeting*, vol.2, pp.1035–1040, 13–18 Oct. 2002.
- [7] K. H. Hussein, I. Muta, T. Hoshino, M. Osakada, "Maximum photovoltaic power tracking: an algorithm for rapidly changing atmospheric conditions," *IEE Proceedings on Generation, Transmission and Distribution*, vol.142, no.1, pp.59–64, Jan 1995.
- [8] K. Harada, G. Zhao, "Controlled power interface between solar cells and AC source," *IEEE Transactions on Power Electronics*, vol.8, no.4, pp.654–662, Oct 1993.
- [9] Fangrui Liu, Shanxu Duan, Fei Liu, Bangyin Liu, Yong Kang, "A Variable Step Size INC MPPT Method for PV Systems," *IEEE Transactions on Industrial Electronics*, vol.55, no.7, pp.2622–2628, July 2008.
- [10] Jiyong Li, Honghua Wang, "A novel stand-alone PV generation system based on variable step size INC MPPT and SVPWM control," *IEEE 6th International Power Electronics and Motion Control Conference IPEMC '09*, pp.2155–2160, 17–20 May 2009.